

THE DENSITY OF THE UNIVERSE

Paolo de Bernardis and Silvia Masi
Dipartimento di Fisica, Universita' La Sapienza, Roma

ABSTRACT

The significance and the measurement of the average density of the Universe is reviewed at introductory level. Current observations of the Cosmic Microwave Background anisotropy measure the density to be critical with an accuracy of the order of 10%.

1 Which density ?

Cosmology studies the Universe at large scales (> 100 Mpc). Building blocks for the visible Universe are the Galaxies. The galaxy distribution is close to homogenous at very large scales (see e.g. ¹⁾ ²⁾). So, as a zero order approximation, Cosmology studies the evolution of a homogeneous medium.

The only force effective at very large scales is gravity, and we believe that the correct theory of gravity is general relativity. For this reason, we will refer

to the mass-energy density of the idealized homogeneous medium when we will speak about the density of the Universe. We need to include all the forms of energy contributing to the stress-energy tensor in Einstein's field equations.

Note that the assumption of a homogenous model is crucial. The density of a fractal distribution of matter, for example, is not even defined.

2 Mass-Energy Density and the Expansion of the Universe

The average mass-energy density is a very important parameter. We know, since Hubble's observations, that the Universe is expanding now. The expansion rate is described by the Hubble constant $H_o \sim 70 \text{ km/s/Mpc}$ ³⁾. The Friedmann model of the Universe describes such a system, solving Einstein's field equation in the isotropic homogeneous case ¹³⁾. The striking result of this General Relativistic analysis is that a static Universe is forbidden. Assuming that only matter and radiation are present, there are three families of solutions: expanding forever, critical, expanding and re-collapsing. The kind of expansion depends on the amount of mass-energy present in the Universe. The critical case, where expansion decelerates to complete rest only for $t \rightarrow \infty$, happens when the kinetic energy of the expansion equals the gravitational energy. We can easily find out the mass-energy density ρ_c required in this case. Consider one galaxy, mass m , at distance r from the origin O. The galaxy will recede with speed $H_o r$ and will feel the gravity of all the matter (mass M) inside the sphere of radius r (the Birkhoff theorem of General Relativity is used here). We have

$$\frac{1}{2}mv^2 = \frac{GMm}{r} \quad (1)$$

and using H_o and the density ρ_c :

$$\frac{1}{2}mH_o^2r^2 = \frac{G\frac{4}{3}\pi r^3\rho_c m}{r} \quad (2)$$

so that

$$\rho_c = \frac{3H_o^2}{8\pi G} \quad (3)$$

This is the critical density, numerically $1.88 \times 10^{-26} h^2 \text{ Kg/m}^3$, where $h = H_o/(100\text{km/s/Mpc})$. If the mass-energy density ρ of the Universe is larger than ρ_c , the expansion decelerates to zero and the Universe collapses after a finite time. If $\rho < \rho_c$, the Universe expands forever. The ratio $\Omega = \rho/\rho_c$ is

called the density parameter. The density of the Universe is decreasing during expansion, and at early times all the solutions come from a state of infinite density, the so called Big-Bang.

There is a paradox in this family of solutions. We measure today, some billion years after the big bang, a value of ρ of the order of ρ_c . This means that in the past ρ had to be incredibly close to ρ_c , otherwise we would not exist, either because the Universe would have already collapsed or because it would be already completely diluted. This is a problem of fine tuning of the initial conditions, well known as the *paradox of flatness*, which cannot be solved in the framework of the standard Hot Big Bang theory. The theory of cosmic inflation in the very early Universe offers a solution to this problem and to several others ⁴⁾.

We live in the present epoch, and we only know the present expansion rate of the Universe, measured by the Hubble constant. To know more about its previous and future evolution we need to measure Ω . Moreover, we need to understand what contributes to it. Let's list all the possible contributions.

In the Universe there is light and there is electromagnetic radiation. A lot of photons (about $400 \gamma/\text{cm}^3$). And a lot of neutrinos. But photons and neutrinos today have a mass-energy density which is negligible with respect to the critical density.

We see stars and interstellar gas and dust. Stars are grouped in galaxies which are grouped in galaxy clusters. Hot gas fills the inter-cluster volume. All this luminous (baryonic) matter accounts at most for about 5% of the critical density: $\Omega_b < 0.05$ (see ⁵⁾ for a review).

We know that there is dark matter, which is needed to explain the dynamics of stars in Galaxies and of galaxies in clusters. This dark matter does not interact with light, and we do not know which particles is made of (cold baryons ? neutrinos ? WIMPS, neutralinos ?) Its density is also largely unknown, but estimates are converging to 20-30% of the critical density ($\Omega_m = \Omega_{DM} + \Omega_b \sim 0.3$) ^{6), 7), 8)}.

An additional possibility is that in the universe there is some quantity of repulsive, dark energy: a form of energy with negative pressure (vacuum energy, or cosmological constant Λ , or quintessence). $\Omega_\Lambda \sim 0.7$ would account for the recent evidence for an accelerated expansion of the universe, coming from the observations of distant supernovae (^{10), 11)}). The possible presence of "dark

energy” is quite important for the evolution of the Universe. At some point, ”dark energy” becomes the dominant form of energy, driving an accelerated expansion even if the curvature is positive. If dark energy turns out to be present, curvature and destiny of the Universe are not related anymore (12).

In summary, our knowledge of the content of the Universe is very poor, and we measure directly only a very little fraction of it. We need a different approach to measure Ω .

3 Mass-Energy Density and the Curvature of the Universe

An independent method is the determination of the geometry of the Universe, by means of the observation of its effects on light propagation. According to General Relativity, the presence of mass and energy curves the space. This was experimentally demonstrated since 1919, by observation of the deflection of light coming from distant stars, and passing close to the mass of the Sun. The same phenomenon is now usual in the images of distant sources by the Hubble Space Telescope 9). These sources are deformed by the presence of mass (galaxies or clusters) on the light path, and are often seen as multiple images of the same source (Gravitational lensing).

The large scale geometry of the Universe is controlled by the average mass-energy density in the same way: its presence curves the background metric of the universe. If $\Omega = 1$, the geometry is the standard Euclidean geometry, the space is not curved, and light rays starting parallel will travel parallel forever. If $\Omega > 1$, the additional mass-energy will curve the space so that the global curvature is positive. Two light rays starting parallel will converge. If $\Omega < 1$, the defect of mass-energy will curve the space so that the global curvature is negative. Two light rays starting parallel will diverge.

We need a method to detect the curvature of light rays due to the background metric of our Universe. It is a small effect locally, so we need to perform the test over cosmological scales. If we could place a standard ruler at very large distance, we could do the test by measuring the angle subtended by the ruler. For $\Omega = 1$ the angle would be the one computed from elementary geometry in an Euclidean space. For $\Omega > 1$, we expect to see a larger angle, because light rays converge towards the observer. For $\Omega < 1$ we expect to see a smaller angle.

The angular size of a source with proper linear size d is $\theta = d/d_A$. In

the Friedmann-Robertson-Walker metric, the angular-diameter distance d_A as a function of the redshift z and of the different density parameters can be derived in closed form (14):

$$d_A = \frac{1}{\Omega_k^{1/2} H_o (1+z)} \sinh \left[\Omega_k^{1/2} \int_{\frac{1}{1+z}}^1 \frac{dx}{\sqrt{\Omega_\Lambda x^4 + \Omega_k x^2 + \Omega_M x}} \right] \quad (4)$$

Here $\Omega_k = 1 - \Omega_M - \Omega_\Lambda = 1 - \Omega$; the sinh function must be used for $\Omega < 1$ and has to be replaced with a sin function for $\Omega > 1$. In principle one could use the diameters of Galaxies as a standard rulers, and infer the Ω s from a best fit to $d_A(z)$. But the diameter of Galaxies is hard to define, and evolution effects are important. High redshift Galaxies tend to be more irregular. Similar evolution problems are present for radio-galaxies. The solution to this problem came recently from the study of the first high resolution images of the Cosmic Microwave Background.

4 The Image of the Cosmic Microwave Background

Since the Universe is expanding, it has been denser and hotter in the past. We have a way to investigate directly early epochs, due to the finite speed of light: looking far away is the same as looking in the past. If we look back far enough, we will see an epoch when the universe was about as hot as the surface of the Sun, at a temperature of several thousand K. Then the universe was a hot plasma, called "the primeval fireball", where photons and matter were in thermal equilibrium, due to Thomson scattering of photons against free electrons. We cannot see earlier epochs - as we cannot see inside the Sun - because the plasma is opaque to light. We expect to see light coming from there. Due to the expansion of the Universe, that visible and near infrared light has been red-shifted by a factor 1000, and is now a faint glow of microwaves: the Cosmic Microwave Background (CMB). This has been detected as a 2.73 K blackbody (16). In the framework of the Hot Big Bang model, when we look to the Cosmic Microwave Background we look back in time to the epoch when temperature decreased below ~ 3000 K for the first time. This is the end of the plasma era, at a redshift ~ 1000 , when the universe was ~ 50000 times younger, ~ 1000 times hotter and $\sim 10^9$ times denser than today. It is a transition epoch (called "recombination"): the ionized, opaque Universe becomes neutral and transparent to light, so that CMB photons can travel freely all the way to our

telescopes . The other very important consequence of the transition regards the evolution of density perturbations ($\Delta\rho/\rho$). Density perturbations were oscillating in the primeval fireball as a result of the opposite effects of the pressure of photons and of gravity. After recombination, photons pressure becomes unimportant, and $\Delta\rho/\rho$ can grow and create, through gravitational instability, the hierarchy of structures we see today in the nearby Universe. There are three physical processes converting the density perturbations $\Delta\rho/\rho$ present at recombination into *observable* CMB temperature fluctuations $\Delta T/T$. They are: the photon density fluctuations δ_γ , which can be related to the matter density fluctuations $\Delta\rho$ once the kind of perturbations is specified; the gravitational redshift of photons scattered in an overdensity or an underdensity with gravitational potential difference ϕ_r (Sachs-Wolfe effect ¹⁵); and the Doppler effect produced by the proper motion with velocity v of the electrons scattering the CMB photons. In formulas:

$$\frac{\Delta T}{T}(\vec{n}) \approx \frac{1}{4}\delta_{\gamma r} + \frac{1}{3}\frac{\phi_r}{c^2} - \vec{n}\frac{\vec{v}_r}{c} \quad (5)$$

where n is the line of sight vector and the subscript r labels quantities at recombination. If we are able to measure an image of the CMB, we can estimate the density fluctuations present in the Universe at recombination, which are the early progenitors of the structures present today in the Universe. Moreover, the density fluctuations present at recombination result from processes in the very early Universe, and the observation of the CMB seems to be a good way to investigate them.

5 A standard ruler at recombination

The fact of interest here is that there is a *characteristic scale* in the CMB anisotropy at recombination, because there is an *acoustic horizon* at recombination. The acoustic horizon is determined by the distance sound waves can travel since the Big Bang. The speed of sound in the primeval plasma is close to the speed of light (basically $c_s = c/\sqrt{3}$). The size of the acoustic horizon increases with time. Density perturbations of a given proper size start to oscillate only when the acoustic horizon encompasses them. As long as they are larger than the acoustic horizon, they just follow the expansion of a slightly over-dense or under-dense universe, and do not oscillate. When the acoustic

horizon becomes larger than their size, the opposite edges of the perturbation begin to feel the effects of the forces, and the acoustic oscillation starts. The size of the horizon at recombination separates perturbations which have never oscillated from those that have undergone acoustic oscillations. Let's focus on perturbations with a size slightly smaller than the acoustic horizon. These perturbations will start the oscillation just before recombination, and will have just enough time to fully compress. They will be evident as slightly hotter or slightly colder spots in the image of the CMB. The age of the Universe at recombination is of the order of 3×10^5 years, so the characteristic proper size of these spots is 3×10^5 light-years. This is the standard ruler we needed at cosmological distances. Perturbations slightly smaller or slightly larger than these will not be fully compressed or rarefied, and will not be as evident as these in the image of the CMB. The distance between us and recombination is of the order of the present age of the Universe, i.e. $\sim 15 \times 10^9$ light years. In an Euclidean Universe, the apparent size of these spots will be simply $\theta \sim 10^3 \times 3 \times 10^5 / 15 \times 10^9$ rad, i.e. about one degree (the factor 10^3 comes from the expansion of the Universe after recombination). If, instead, the geometry of the Universe is not Euclidean ($\Omega \neq 1$), then we expect to see magnified spots ($\theta > 1^\circ$) if $\Omega > 1$, and de-magnified spots ($\theta < 1^\circ$) if $\Omega < 1$. The recipe for this measurement is thus:

- Take a picture of the CMB with sufficient angular resolution, $\Delta T(\alpha, \delta)$.
- Compute the angular power spectrum of the image, c_ℓ . Here $c_\ell = \langle |a_{\ell, m}|^2 \rangle$, where $\Delta T(\alpha, \delta) = \sum_{\ell, m} a_{\ell, m} Y_m^\ell(\alpha, \delta)$.
- Check if there is a peak at multipoles corresponding to an angular scale of the order of 1° ($\ell \sim \pi/\theta \sim 200$). The value of Ω will be determined by the location of the peak (i.e. the typical projected angular size of the spots).

The qualitative analysis above can be made rigorously (see e.g. 17), 18), 19). The result is that the location of the first peak in the angular power spectrum of the CMB is indeed a strong function of Ω , but also of Ω_M (or Ω_Λ) 18). In the region $\Omega \sim 1$, it results $\ell_p \sim \Omega^{-\nu}$, with $\nu \sim 2.2, 1.6, 1.25, 0.4$ if $\Omega_M \sim 0.2, 0.3, 0.4, 1$.

There is a lot more information encoded in the angular power spectrum of the CMB (see 20) for a recent review). Multiple peaks are present in the spectrum. The relative amplitudes are sensitive to the physical density of baryons $\Omega_b h^2$, and to the initial power spectrum of the density fluctuations.

This is usually parametrized as $\Delta\rho/\rho(k) \sim k^n$ (here k is the wavenumber, i.e. the inverse of the physical wavelength of the perturbation). Inflationary models ⁴⁾ naturally produce adiabatic, gaussian density fluctuations, with a power spectrum with $n \sim 1$. To a lesser extent, the angular power spectrum of the CMB is also sensitive to other cosmological parameters, like the reionization optical depth τ_C , the different mass-energy densities, and the Hubble constant. The main purpose of the space missions MAP ²¹⁾ and Planck ²²⁾ is the measurement of the power spectrum of the CMB with sufficient resolution and accuracy to allow a precision measurement of all the cosmological parameters.

6 Measuring the Image of the Cosmic Microwave Background

The hunt for detecting anisotropies in the CMB and possibly build an image of it started in the 70s. The CMB turns out to be extraordinarily isotropic: apart from the dipole component due to the motion of the Earth, it became clear soon that any intrinsic anisotropy had to be smaller than 100 parts per million. Measurements are extremely difficult, due to the small amplitude of the anisotropy and to the variability of the atmospheric emission, which is much larger than the signal to be measured. Measurements must be carried out either in the microwaves, from cold, dry sites, or in the far infrared, outside the earth atmosphere, using stratospheric balloons, rockets and satellites. After 27 years of pioneering efforts, the COBE satellite of NASA produced the first detection in 1992. The DMR instrument aboard of the COBE satellite measured the first map of CMB anisotropy ²³⁾. Due to the coarse angular resolution of the instrument ($\sim 7^\circ$ FWHM), only large scale structures could be detected. The contrast of the resulting image is very low, but there are structures, at a level of 10 ppm: $\Delta T_{rms} = (30 \pm 3)\mu K$. The consequence of this observation is that the early universe is smooth at large scales. This is not trivial, because of causal horizon effects: regions of the sky distant more than $\sim 1^\circ$ are not in causal contact at recombination. Why regions many degrees apart feature the same temperature, within a few tens of ppm? This is called the paradox of horizons, and has been solved only with the inflation theory. The angular power spectrum of the CMB was measured for $\ell < 20$ and is consistent with the Harrison-Zeldovich power spectrum $P(k) = Ak^n$ with $n = (1.0 \pm 0.3)$ ²⁴⁾. This is consistent with the predictions of the inflation theory. The resolution of COBE was not enough to make the measurement of Ω outlined above, which requires

an angular resolution better than 1° FWHM. In a long lasting experimental effort, the degree-scale and sub-degree-scale anisotropy has been detected by several ground based and balloon-borne experiments. Only recently, however, it has been possible to detect the presence of peaks in the power spectrum (25), (26), (27), and to produce images where the sub-degree anisotropy is clearly visible (28), (29), (30), (31).

Let's focus now on the BOOMERanG experiment, which produced the first wide sky maps where sub-horizon structures in the CMB are detected with high confidence (28). The instrument setup has been described in detail in (35), (36), (37). It is a scanning telescope, featuring important improvements with respect to previous experiments. First, BOOMERanG uses a long duration (7 to 14 days) stratospheric (~ 38 km) balloon flight around Antarctica. Long integrations on a wide sky region are obtained, along with careful and extensive tests for systematic effects. In addition, flying during the austral summer from Antarctica, the lowest Galactic contamination region of the sky (38) is visible at an azimuth almost perfectly opposite to the azimuth of the Sun. This simplifies the necessary shielding required for thermal and optical reasons. Second, BOOMERanG uses a very sensitive total power receiver, based on spider-web bolometers (39) cooled to 0.28 K with a custom cryogenic system (40), (41). The power detected from one direction is compared to the power from contiguous directions by slowly scanning the telescope ($1^\circ/s$ to $2^\circ/s$ in azimuth). This strategy is enabled by the intrinsic stability of the readout electronics (a low noise AC bridge) and of the detectors. The full payload is gently moved, avoiding mechanical choppers and the related inefficiencies and slowly varying offsets. Third, the focal plane is multiband, with 8 pixels and 4 colors (90, 150, 240, 410 GHz) strategically located with respect to the scan direction in order to have several temporal and spectral confirmations of the detected structures. We track the azimuth of the best sky region while scanning at constant elevation, thus obtaining highly cross-linked maps. BOOMERanG has obtained maps of about 3% of the sky at the four frequencies, with angular resolution ranging between 18 and 12 arcmin for the different channels. The structure evident in the maps at 90, 150 and 240 GHz is spectrally consistent with CMB anisotropy, strongly excluding a local origin of the detected temperature fluctuations (42). The power spectrum has been estimated from the central part of the map, corresponding to about 1% of the sky in (28) and 1.8% of the sky in

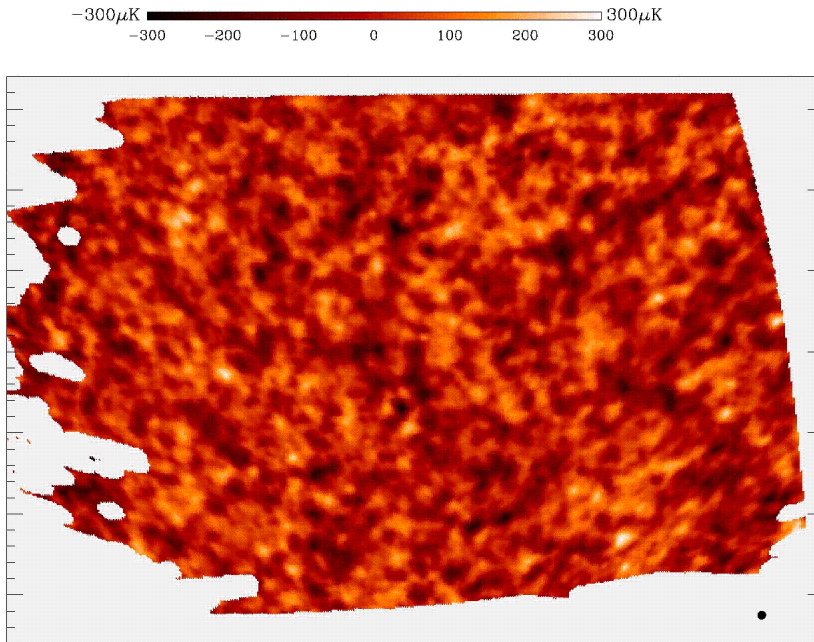


Figure 1: *Map of about 3% of the sky obtained at 150 GHz from one of the BOOMERanG detectors. The black disk has a diameter of 0.5° . The structures dominating the figure are temperature fluctuations of the Cosmic Microwave Background due to acoustic oscillations in the primeval plasma. The rms amplitude of the fluctuations is $\sim 80\mu K$, while the characteristic size of the hot and cold spots is $\sim 1^\circ$.*

30). The map derived from one 150 GHz channel is visible in fig.1. Multiple peaks are evident in the angular power spectrum ³²⁾, the first one located at $\ell \sim 210$. The presence of multiple peaks is the confirmation of the presence of acoustic oscillations in the plasma before recombination, and allows the detection of several important cosmological parameters ³²⁾, ³³⁾, ³⁴⁾. Ω is detected by measuring the location of the first peak. The angular power spectrum of the CMB detected by BOOMERanG ²⁸⁾, ³⁰⁾, DASI ³¹⁾ and MAXIMA ²⁹⁾, ³¹⁾ is plotted in fig.1. Given the orthogonality of the experimental and analysis methods, the agreement of the three results is very good, at least visually. The existing anti-correlations in the bandpowers, and the presence of some overlap

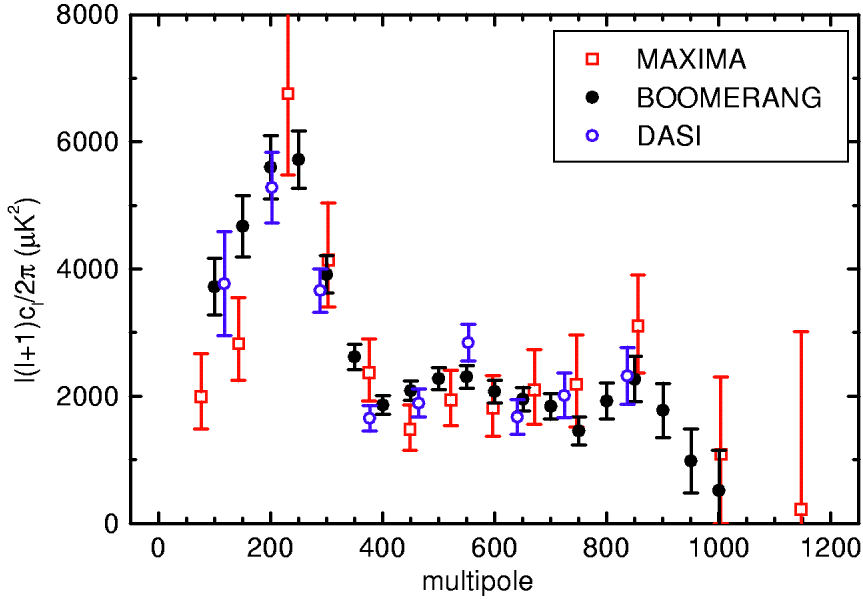


Figure 2: CMB anisotropy power spectrum detected by BOOMERanG, MAXIMA and DASI. Approximately uncorrelated bandpowers are plotted for each of the experiments. The error bars represent statistical errors only. A peak at $\ell \sim 200$ is evident in all datasets. This is a strong indication of a critical density of the Universe.

in the sky coverage of the BOOMERanG and DASI data should be taken into account for a more quantitative comparison. Such a comparison will be the best argument to exclude significant systematic effects in the three spectra.

7 Measuring Ω from the power spectrum

ℓ_{peak} has been evaluated from the BOOMERanG data by means of a quadratic fit to the power spectrum. We find $\ell_1 = (213^{+10}_{-13})$ ³². In the framework of inflationary adiabatic cold dark matter models this location of the peak strongly suggests a flat geometry of the Universe. More accurate statements require a through analysis of the full power spectrum dataset. A bayesian likelihood

analysis has been carried out in order to constrain instrumental and cosmological parameters given the measured power spectrum, the COBE power spectrum data at low multipoles, and a set of prior distributions for the parameters. A database of power spectra, for several millions of cases with different combinations of the values of the cosmological parameters, has been computed. The ranges and sampling selected for each parameter are wide enough to cover in detail the relevant parameters space. For each model the likelihood of the data, given the model and the assumed prior distributions, has been computed. Uniform prior distributions for all the assumed parameters have been used. The results obtained from the data of ³⁰⁾ are robust with respect to changes in the priors. Using only the prior $0.45 < h < 0.9$, the Bayesian determination of Ω is $\Omega = 1.02^{+0.05}_{-0.06}$. This result comes from a marginalization over all the other parameters and over the uncertainties in the gain calibration and in the beam FWHM. This determination of Ω definitely points towards a Euclidean geometry of our Universe. The BOOMERanG result above is in very good agreement with the independent determinations of DASI ($\Omega = 1.04 \pm 0.06$) ³³⁾ and MAXIMA ($\Omega = 0.90 \pm 0.15$) ⁴³⁾.

The extension of the multipoles coverage up to $\ell \sim 1000$ allows breaking the important degeneracy between $\Omega_b h^2$ and n . From BOOMERanG $\Omega_b h^2 = 0.022^{+0.004}_{-0.003}$ and $n_s = 0.96^{+0.10}_{-0.09}$. The quality of the data is so good that just the addition of the weak prior on h allows breaking the degeneracy between Ω_Λ and Ω_M . We find $\Omega_\Lambda = 0.51^{+0.23}_{-0.20}$ and $\Omega_{DM} h^2 = 0.13 \pm 0.05$. The addition of either a prior on the large scale structure (through the parameters σ_8 and Γ) or a prior on the SN1a observations, or even just a more restrictive prior on $h = 0.71 \pm 0.08$ produce very significant detections of Ω_Λ : $\Omega_\Lambda = (0.55 \pm 0.09)$, $(0.73^{+0.07}_{-0.10})$, $(0.62^{+0.10}_{-0.18})$ respectively ³⁰⁾, ³²⁾.

8 Conclusions

The CMB anisotropy experiments have recently resolved horizon and sub-horizon structures at recombination. Their typical size is $\sim 1^\circ$, strongly suggesting a Universe with Euclidean geometry and critical density. The density of the Universe has significant contributions from dark energy (about 70%), dark matter (about 25%) and baryons (less than 4%). Independent cosmological observations point to this unexpected composition of the Universe. Understanding the nature of dark matter and dark energy is now the most important

goal of cosmological research.

9 Acknowledgements

This work has been supported by ASI, PNRA and University of Rome La Sapienza. The BOOMERanG program has also been supported in USA by NSF and NASA, in UK by PPARC, and by CIAR and NSERC in Canada. We thank the organizers of the ISSS for wonderful hospitality.

References

1. J.E. Peebles *et al.*, Principles of Physical Cosmology, Princeton University Press, (1993).
2. J.A. Peacock, Cosmological Physics, Cambridge University Press, (1999).
3. W. Freedman, in "David Shramm memorial volume", Physics Reports, astro-ph/9909076, (2000).
4. E.W. Kolb and Turner M.S, The Early Universe, Addison-Wesley, (1990).
5. Fukugita *et al.*, Ap.J. **503**, 518 (1998).
6. Bahcall *et al.*, astro-ph/9906463 (1999).
7. Wittman *et al.*, Nature **405**, 143 (2000).
8. R. Juskiewicz *et al.*, Science **287**, 109 (2000).
9. <http://opposite.stsci.edu/pubinfo/pr/2000/08/pr-photos.html>
10. A.G. Riess *et al.* Ap.J. **116**, 1009 (1998).
11. S. Perlmutter *et al.*, Nature **391**, 51 (1998).
12. L.M. Krauss, M.S. Turner, Gen.Rel.Grav. **31**, 1453 (1999).
13. Weinberg S., Gravitation and Cosmology, (1981).
14. Peebles P.J.E, Principles of Physical Cosmology, Princeton Series in Physics, (1994).
15. Sachs R.K., Wolfe, A.M., Ap.J. **147**, 73 (1967).

16. Mather J. *et al.*, Ap.J. **354**, L37 (1990).
17. Bond D., and Efstathiou G., astro-ph/9807103, (1998).
18. Weinberg S., astro-ph/0006276, (2000).
19. Melchiorri A., and Griffith, X, astro-ph/0011147, (2000).
20. Hu W., and Dodelson A., Ann.Rev.Astron.Astrophys., astro-ph/0110414, (2002).
21. <http://map.gsfc.nasa.gov>
22. <http://astro.estec.esa.nl/Planck>
23. G. Smoot *et al.*, Ap.J. **396**, L1 (1992).
24. C. Bennett *et al.*, Ap.J. **464**, L1 (1996).
25. A. Miller *et al.*, Ap.J. **524**, L1 (1999).
26. E. Torbet *et al.*, Ap.J. **521**, L79 (1999).
27. P. Matuszewska-Janusz *et al.*, Ap.J. **536**, L59 (2000).
28. P. de Bernardis *et al.*, Nature **404**, 955-959 (2000).
29. S. Hanany *et al.* Ap.J. **545**, L5 (2000).
30. B. Netterfield *et al.* submitted to Ap.J., astro-ph/0104460, (2001).
31. E.M. Leitch *et al.* astro-ph/0104488 (2001).
32. P. de Bernardis *et al.*, Ap.J. in press, astro-ph/0105296 (2002).
33. C. Pryke *et al.*, astro-ph/0104490 (2002).
34. A.T. Lee *et al.*, astro-ph/0104459 (2001).
35. S. Masi *et al.*, in "3K cosmology", AIP Conf. Proc. 476, 237 (1999); astro-ph/9911520
36. B.P. Crill Ph.D. thesis, Caltech. (2000).
37. F. Piacentini *et al.* astro-ph/0105148

38. D.J. Schlegel *et al.*, *Ap.J.* **500**, 525 (1998).
39. P. Mauskopf *et al.*, *Appl.Opt.* **36**, 765 (1997).
40. S. Masi *et al.*, *Cryogenics* **38**, 319 (1998).
41. S. Masi *et al.*, *Cryogenics* **39**, 217 (1999).
42. S. Masi *et al.*, *Ap.J.* **553**, L93 (2001).
43. A. Balbi *et al.* astro-ph/0005124, (2001).